SARTORIUS

Application Note

November 1, 2024

Keywords or phrases:
Adeno-associated virus, monolithic chromatography, purification, downstream processing, gene therapy, CIMmultus®, MODDE®

Robust and Scalable AAV8 Purification: A Two-Step Monolithic Chromatography Process

Franziska Bollmann[1,*], Marc Noverraz[2], Geoffrey Pressac[3]

[1]Sartorius Stedim Biotech GmbH, 37079 Göttingen, Germany
[2]Sartorius Stedim Switzerland AG, 8317 Tagelswangen, Switzerland
[3]Sartorius Stedim France S.A.S., 13400 Aubagne, France

*Correspondence
Email: franziska.bollmann@sartorius.com

Abstract

This study explores monolithic chromatography as an alternative to conventional resin- and ultracentrifugation-based methods for purifying adeno-associated viruses (AAVs). Leveraging monoliths' convective mass transport for high resolution and capacity, lower pressure drops, higher flow rates, and reusability, we implemented a two-step approach for AAV8 purification, using CIMmultus® SO3 for initial capture and trialing three different chemistries (CIMmultus® QA, CIMmultus PrimaS®, and CIMmultus® PrimaT) for polishing. A design of experiments approach optimized the capture process, while the polishing steps effectively separated empty and full capsids, achieving high recovery and impurity clearance, including empty capsids. The scalability of the process was demonstrated, showcasing the robustness and efficiency of monolithic chromatography as a scalable alternative to conventional AAV purification.

For further information, visit
sartorius.com/monolithic-chromatography

Introduction

Adeno-associated virus (AAV) vectors are at the forefront of gene therapy delivery[1]. Consequently, there is an urgent need to enhance both upstream titers and downstream efficiencies in the AAV production process to meet current and future market demands[2]. Affinity capture chromatography is a widely used method for AAV purification, with commercially available resins offering high binding capacity and suitability for various serotypes, achieving respectable recovery rates and robust impurity clearance[3,4]. However, affinity chromatography has limitations, including harsh elution conditions, low flow rates, and lack of universality across serotypes. Post-capture, the removal of empty AAV capsids, which do not contain viral DNA, is necessary to improve potency and reduce immunogenicity[5]. Currently, gradient ultracentrifugation (using cesium chloride or iodixanol) is the gold standard for separating empty and full AAV capsids[3,6], but its scalability and purity challenges limit productivity.

Monolithic chromatography presents a viable alternative to conventional purification strategies. Mass transport in monoliths is exclusively convective, enabling flow-independent resolution and capacity. Monoliths also benefit from lower pressure drops, higher flow rates, increased mechanical strength, reduced costs, and reusability[7,8]. Their well-defined and interconnected channel structure results in high binding capacities, and the convective mass transport enables high resolution, which is particularly important for differentiating between empty and full AAV capsids during polishing[9].

We implemented a two-step monolithic chromatography approach for the purification of AAV8, employing higher flow rates compared to traditional resin chromatography. A design of experiments (DoE) approach was employed to optimize process parameters specifically for capture with CIMmultus® SO3, a cation-exchange monolith. We then tested three distinct chemistries for polishing: an anion-exchange (CIMmultus® QA) and two multimodal (CIMmultus PrimaS® and CIMmultus® PrimaT). CIMmultus® QA is functionalized with a quaternary amine and serves as a strong anion-exchange monolith. CIMmultus PrimaS® captures AAVs through both hydrogen-bonding and weak anion exchange, while CIMmultus® PrimaT interacts through weak anion exchange, hydrogen bonding, and metal chelation effects[10]. After establishing the processes, we scaled them up.

Materials and Methods

Full methods are available in[11] and described briefly below. The AAV8 production process is illustrated schematically in Figure 1.

Figure 1: *Schematic of the 15 L Production Process Used to Generate AAV8 Material for the Study*

1 Upstream Production
- 20 L stirred-tank bioreactor
- Suspension-adapted HEK293T cells
- Triple transfection

2 Lysis and Nuclease Digestion
- Tween-20 (1% v/v)
- Benzonase (50 units/mL)

3 Clarification
- Sartoclear® DL75
- Sartopore® 2 XLG

4 Concentration
- Sartocon® Slice PESU 100 kDa
- 10-fold concentration
- 5 diafiltration volumes

5 pH Titration and Filtration
- Titration to pH 3.5, 4, or 4.5
- 0.45 µm filtration

6 Capture Chromatography
- CIMmultus® SO3

7 Dilution or Buffer Exchange
- Dilution for CIMmultus® QA
- Buffer exchange for CIMmultus PrimaS® and PrimaT

8 Polishing Chromatography
- CIMmultus® QA
- CIMmultus PrimaS®
- CIMmultus® PrimaT

AAV8 Production, Lysis, Clarification, and Concentration

HEK293T cells cultured in a 20 L stirred tank bioreactor were transfected with pRC8 (Addgene), pAAV-GFP (PlasmidFactory), and pHelper (Addgene) plasmids. PEIpro® (Polyplus, now part of Sartorius) was used as a transfection reagent. Cells were lysed 72 h after transfection and then subject to nuclease treatment. The cell lysate was clarified with a Sartoclear® DL75 depth filter (Sartorius) followed by Sartopore® 2 XLG 0.8|0.2 µm (Sartorius)[12]. The clarified AAV8 was concentrated ten times and subject to five diafiltration volumes using a Sartocon® Slice PESU 100 kDa flat sheet membrane (Sartorius)[13].

Chromatography and Sample Preparation

CIMmultus® SO3: Chromatographic runs were performed using 1 mL CIMmultus® SO3 monoliths (8 mL for scaled-up runs) with an ÄKTA avant™ (Cytiva) system. AAV8 samples were diluted, pH-adjusted, and filtered before loading. Samples were loaded to achieve the target viral genome (vg) amount per monolith volume, followed by washing, elution, and collected peaks were neutralized immediately. Flow rates of 5 Monolith Volumes (MV)/min were applied, except during cleaning (0.5 MV/min). Composition of load and elution buffer are listed in Table 1.

Table 1: *Composition of Load and Elution Buffer for All Monoliths Evaluated*

Monolith	Load Buffer (A)	Elution Buffer (B)
CIMmultus® SO3	50 mM acetate (except for using glycine if the target pH was 3.5), 50 mM NaCl, 0.01% (w/w) Poloxamer 188, 2 mM $MgCl_2$. pH 3.5, 4.0, or 4.5	Same composition as load buffer + 2 M NaCl
CIMmultus® QA	10 mM Bis Tris Propane, 0.01% (w/v) Poloxamer 188, 1% Sucrose, 5 mM $MgCl_2$ at pH 8.5	10 mM Bis Tris Propane, 0.01% (w/v) Poloxamer 188, 1% Sucrose, 5 mM $MgCl_2$, 0.5 M NaCl at pH 8.5
CIMmultus PrimaS®	10 mM Tris, 10 mM Bis Tris Propane, 0.01% (w/v) Poloxamer 188, 1% Sucrose, 2 mM $MgCl_2$, pH 7	10 mM Tris, 10 mM Bis Tris Propane, 0.01% (w/v) Poloxamer 188, 1% Sucrose, 2 mM $MgCl_2$, pH 9.5
CIMmultus® PrimaT	**A1:** 25 mM HEPES, 0.01% (w/v) Poloxamer 188, 1% Sucrose, pH 7.0 **A2:** 50 mM Tris, 13.6 mM borate, 0.01% (w/v) Poloxamer 188, 1% Sucrose, pH 9	**B1:** 50 mM Tris, 9.6 mM borate, 50 mM $MgCl_2$, 0.01% (w/v) Poloxamer 188, 1% Sucrose, pH 9 **B2:** 50 mM Tris, 12 mM borate, 2 M NaCl, 0.01% (w/v) Poloxamer 188, 1% Sucrose, pH 9

A two-factor, two-level, full-factorial DoE was conducted with buffer pH (3.5 to 4.5) and vg load amount (4.9×10^{12} to 1.2×10^{13} vg/mL$_{(monolith)}$) as factors, including three center-point replicates to check for variability. The DoE was designed with the software MODDE® (Sartorius). A linear gradient elution was applied for the initial DoE study, and the process was later transferred to a step elution (applied to the scale-up study). The statistical models for the experimental responses were analysed using MODDE® v13. The model analysis included an analysis of the importance of model coefficients. All coefficients included within the models had a p-value <0.05 (unless they were included to hierarchy for interaction terms), indicating their inclusion in the model was significant. The overall model accuracy and fit for purpose was assessed by looking at the descriptive power (indicated by a high R^2) and the predictive power (indicated by a high Q^2).

CIMmultus® QA: The loading sample was conditioned through dilution to achieve a low conductivity (2–5 mS/cm) and a pH of 8.5, to ensure maximum AAV binding. AAV8 samples, targeting 1×10^{13} vg/mL$_{(monolith)}$, were loaded onto 1 mL CIMmultus® QA monoliths, followed by washing and gradient elution using a 60 MV linear salt gradient transitioning from low to high NaCl (refer to Table 1 for buffer compositions). Peaks were collected and neutralized. Flow rates of 5 MV/min were applied, except during elution (2 MV/min) and cleaning (0.5 MV/min).

CIMmultus PrimaS®: Following capture with CIMmultus® SO3, the AAV8 sample was diafiltrated with CIMmultus PrimaS® loading buffer to prevent AAV8 loss during loading. AAV8 samples, targeting 1×10^{13} vg/mL$_{(monolith)}$, were loaded onto 1 mL CIMmultus PrimaS® monoliths, followed by washing and elution with a linear pH gradient from 7.5 to 9.5 over 50 MV (refer to Table 1 for buffer compositions). Peaks were collected. Flow rates of 5 MV/min were applied, except during elution (2 MV/min) and cleaning (0.5 MV/min).

CIMmultus® PrimaT: The loading sample was diafiltrated with the load buffer A1, following a similar procedure to that of CIMmultus PrimaS®. AAV8 samples, targeting 1×10^{13} vg/mL$_{(monolith)}$, were loaded onto 1 mL CIMmultus® PrimaT monoliths (4 mL for scaled-up runs), followed by a washing step with buffer A1. Then, a pH shift from 7.0 to 9.0 was performed using load buffer A2, followed by a $MgCl_2$ gradient elution over 20 MV with buffer B1 and a high salt strip with buffer B2. Peaks were collected. Flow rates of 5 MV/min were applied, except during elution (2 MV/min) and cleaning (0.5 MV/min).

Analytical Methods

Particle Quantification

Total AAV8 particles (TP) were quantified using an AAV8 ELISA assay (Progen Biotechnik) according to the manufacturer's instructions. A four-parameter logistic model was applied to quantify the total particle concentration, based on the absorbances at 450 nm of the several standard dilutions. Viral genome titer was evaluated by real-time qPCR.

Empty and Full Particle Determination

PATfix® Anion-Exchange Analysis: Chromatographic analyses were performed on a PATfix® liquid chromatography (LC) system and CIMac AAV (Sartorius) analytical columns. The flowrate used was 1 mL/min. Empty and full AAV8 peaks were integrated in the PATfix® software using a deconvolution function, with a prior subtracted signal baseline.

Mass Photometry (MP) Analysis: Mass photometry was carried out to determine the empty | full particle ratio using SamuxMP (Refeyn) with the Refeyn AcquireMP and Refeyn EvaluateMP software. The samples were diluted to a concentration between 1×10^{10} and 1×10^{11} total AAV8 particles.

Total Protein and dsDNA Analysis: Total protein quantification was done using a BCA Protein Assay Kit (Thermo Fisher Scientific). Total dsDNA was measured using a Quant-iT™ Picogreen® dsDNA assay kit (Invitrogen). λ-DNA was used to construct a calibration curve.

Results

Optimization of AAV8 Capture Chromatography Using CIMmultus® SO3

CIMmultus® SO3 (cation exchanger) was used to purify AAV8 by removing major impurities, such as DNA and proteins. Employing a DoE approach, key parameters, such as the pH of the buffer system and the loaded vg amount/mL of the monolith, were varied systematically to determine the optimal conditions to maximize AAV purity and recovery (Figure 2A).

The analysis of the results and subsequent modeling analysis of the DoE revealed that, only the buffer pH significantly impacted vg recoveries, with higher vg recovery at higher buffer pH values (up to 87% at pH 4.5). The loaded vg amount per mL of monolith was deemed insignificant and omitted from the resultant model for vg recoveries. For the model of vg recovery R^2 was 0.7 and Q^2 was 0.4 indicating an acceptable model fit. For impurity removal, we observed higher DNA reduction at lower buffer pH values, and generally low residual protein amounts, independent of the buffer pH (Figure 2A). We observed an R^2 of 0.94 and 0.97 and a Q^2 of 0.17 and 0.61 for residual DNA and protein, respectively, again indicating an acceptable model fit.

Given the priority of maximizing product recovery and virus load over impurity removal during the capture step, a combination of pH 4.5 and vg load of 1.23×10^{13} vg/mL of monolith was selected, falling within a favorable range for protein reduction but less favorably for DNA reduction.

Evaluation of Isocratic Versus Gradient Elution on CIMmultus® SO3

As shown in the previous section, a linear gradient elution (0% to 100% elution buffer) was employed to identify critical process parameters (CPPs) and establish optimal operating conditions. However, for large-scale manufacturing, step elution is frequently preferred due to its simplicity and efficiency. We defined two elution steps at 20% and 100% of the elution buffer (Figure 3B). There are no significant differences between the two different elution strategies for vp and vg recoveries (Figure 3C). However, with step elution, only 16% of the DNA is present after the capture step, in contrast to 82% in the gradient elution. Considering the higher impurity removal and lower elution volume while maintaining AAV8 recovery, we decided to pursue step elution for AAV8 capture using CIMmultus® SO3.

Monolithic Polishing Chromatography for the Separation of Empty and Full AAV8 Capsids

We evaluated the capabilities of three monoliths with distinct binding chemistries in polishing AAV8: CIMmultus® QA, CIMmultus PrimaS®, CIMmultus® PrimaT.

Figure 2: *DoE-Driven Optimization of AAV8 Capture by CIMmultus® SO3*

A

Experiment Number	pH	vg Load	vg Recovery (%)	vp Recovery (%)	Residual DNA (%)	Residual Protein (%)
1	3.5	4.9×10^{11}	41	82	62	20
2	4.5	4.9×10^{11}	87	67	66	32
3	3.5	1.2×10^{13}	36	66	63	2
4	4.5	1.2×10^{13}	64	73	82	4
5	4.0	6.4×10^{12}	47	68	87	0
6	4.0	6.4×10^{12}	46	61	90	0
7	4.0	6.4×10^{12}	46	65	89	1

B

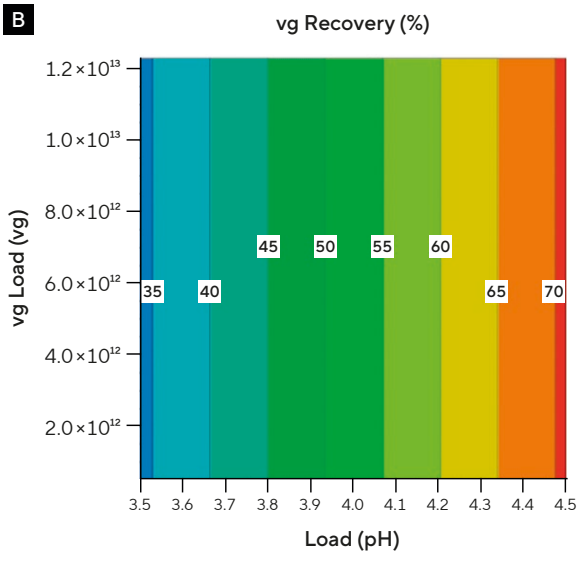

Note. **(A)** Overview of the experimental design factors and ranges evaluated during the DoE to optimize AAV8 capture using CIMmultus® SO3 and the results obtained during the DoE.
(B) Response contour-plot for viral genome recovery resulting from the DoE.

Figure 3: *Comparison of Gradient and Step Elution Operation of CIMmultus® SO3*

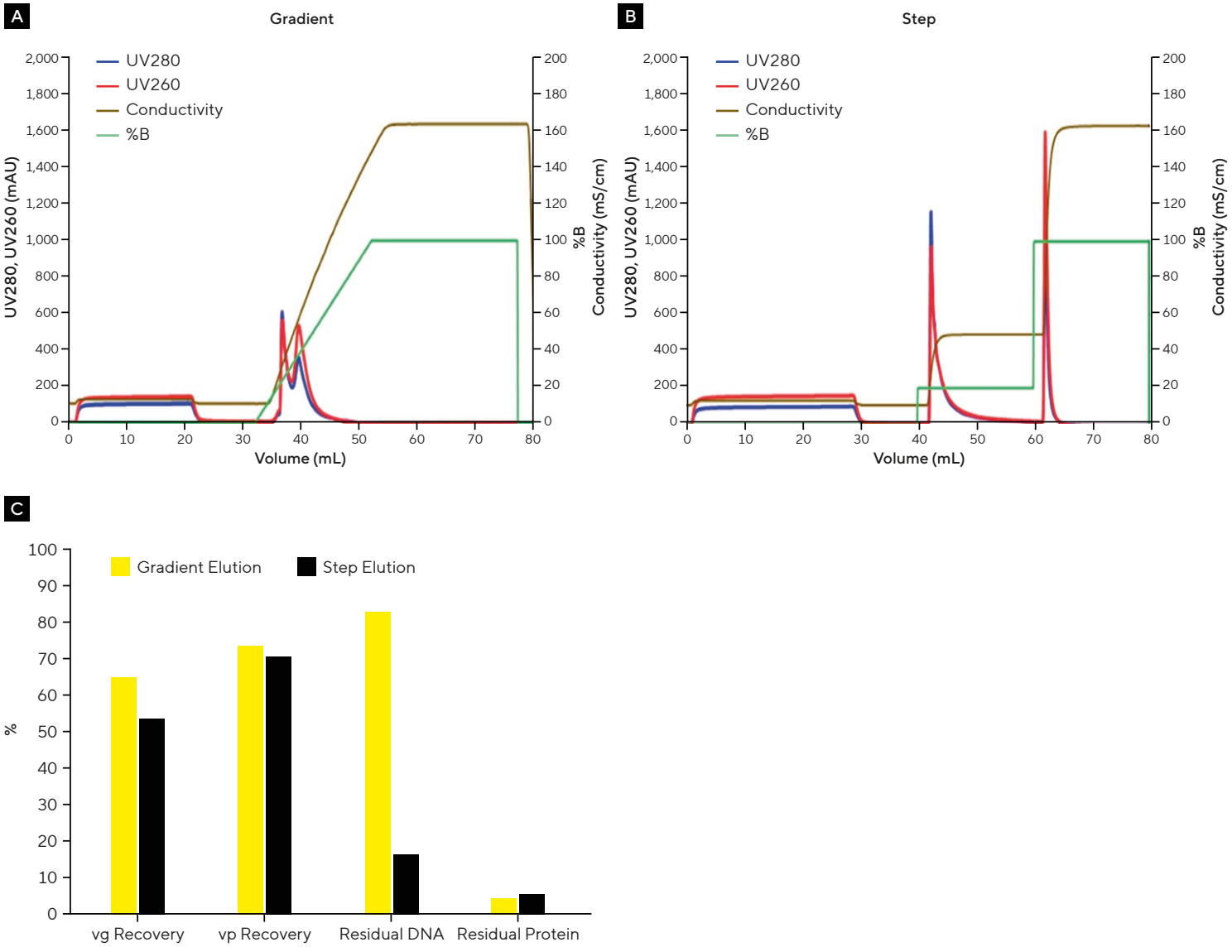

Note. **(A)** Chromatogram of gradient elution method.
(B) Chromatogram of step elution method.
(C) Comparison of analytical assay results between the two elution modes.

Anion-Exchange Chromatography With CIMmultus® QA

The first polishing experiment was carried out using CIMmultus® QA, a strong anion-exchanger, for separation based purely on charge differences between the full and empty capsid species. The absence of a high UV280 signal in the flow-through in the chromatogram indicates that the applied dilution was sufficient, and all AAV8 successfully bound to the monolith (Figure 4A). The gradient elution resulted in two elution peaks. The first peak exhibited a higher UV280 (protein) than UV260 (DNA) signal, while the second peak had a higher UV260 than UV280 signal, strongly indicating successful empty-full separation. The majority of empty AAV8 capsids (E) eluted in the first peak, and the full AAV8 capsids (F) eluted in the second. Analytical results confirmed the efficacy of empty and full AAV8 separation (Table 2).

By isolating the empty AAV8 particles predominantly present in the first elution peak, we increased the full AAV8 population in the second elution peak from 25% after the capture step to over 73% determined by MP (Table 3), or from 34% to 79% determined with PATfix®, respectively. The applied long gradient facilitated good peak resolution, allowing for the independent collection of the two peaks. Furthermore, we achieved over 97% recovery of full AAV8 in the second peak, with only 5% present in the first elution peak. Additionally, the values of DNA and protein present in the full particle elution peak are close to the limit of detection of the analytical techniques, demonstrating the efficiency of CIMmultus® QA in removing not only empty capsids but also contaminating DNA and protein.

Multimodal Chromatography With CIMmultus PrimaS®

Multimodal chromatography uses multiple forms of interaction between solutes and the stationary phase to enhance selectivity. In this study, CIMmultus PrimaS® (which employs hydrogen bonding and weak anion exchange), was used to polish AAV8. After gradient elution, two elution peaks were detected. These had the same UV trend as those from CIMmultus® QA purification, with a shift of UV280 and UV260 signals occurring between elution peaks (Figure 4B), indicating an empty-full separation. The results obtained using CIMmultus PrimaS® are consistent with those of CIMmultus® QA in terms of virus recovery, full particle enrichment, and impurity removal (Table 2 and 3).

This method resulted in high AAV8 recovery, effectively removed protein and DNA impurities, and enriched full particles, with a percentage of full particles of over 80% (MP) or 93% (PATfix®), respectively.

Table 2: *Analytical Assay Results of the AAV8 Polishing Runs Using Three Monoliths With Different Chemistries*

Molonlith	Peak (See Figure 4)	vg Recovery (%)	vp Recovery (%)	DNA (ng/1 × 10^{13} vg)	Proteins (mg/1 × 10^{13} vg)
CIMmultus® QA	E	5.0 ± 0.8	58 ± 10	704 ± 245	42 ± 9
	F	97 ± 9	35 ± 5	37 ± 7	2.4 ± 0.1
CIMmultus PrimaS®	E	3.2 ± 0.2	44 ± 4	1,687 ± 1,026	54 ± 7
	F	78 ± 36	27 ± 10	68 ± 36	5 ± 5
CIMmultus® PrimaT	E	1.7 ± 0.4	65 ± 3	99,572 ± 12,009	28 ± 3
	F	119 ± 2	24 ± 1	115 ± 158	0.5 ± 0.1

Note. E = empty particle peak, F = full particle peak. Mean (N = 2) ± Std Dev

Figure 4: *Chromatograms From AAV8 Polishing Runs With* ***(A)*** *CIMmultus® QA,* ***(B)*** *CIMmultus PrimaS®, and* ***(C)*** *CIMmultus® PrimaT*

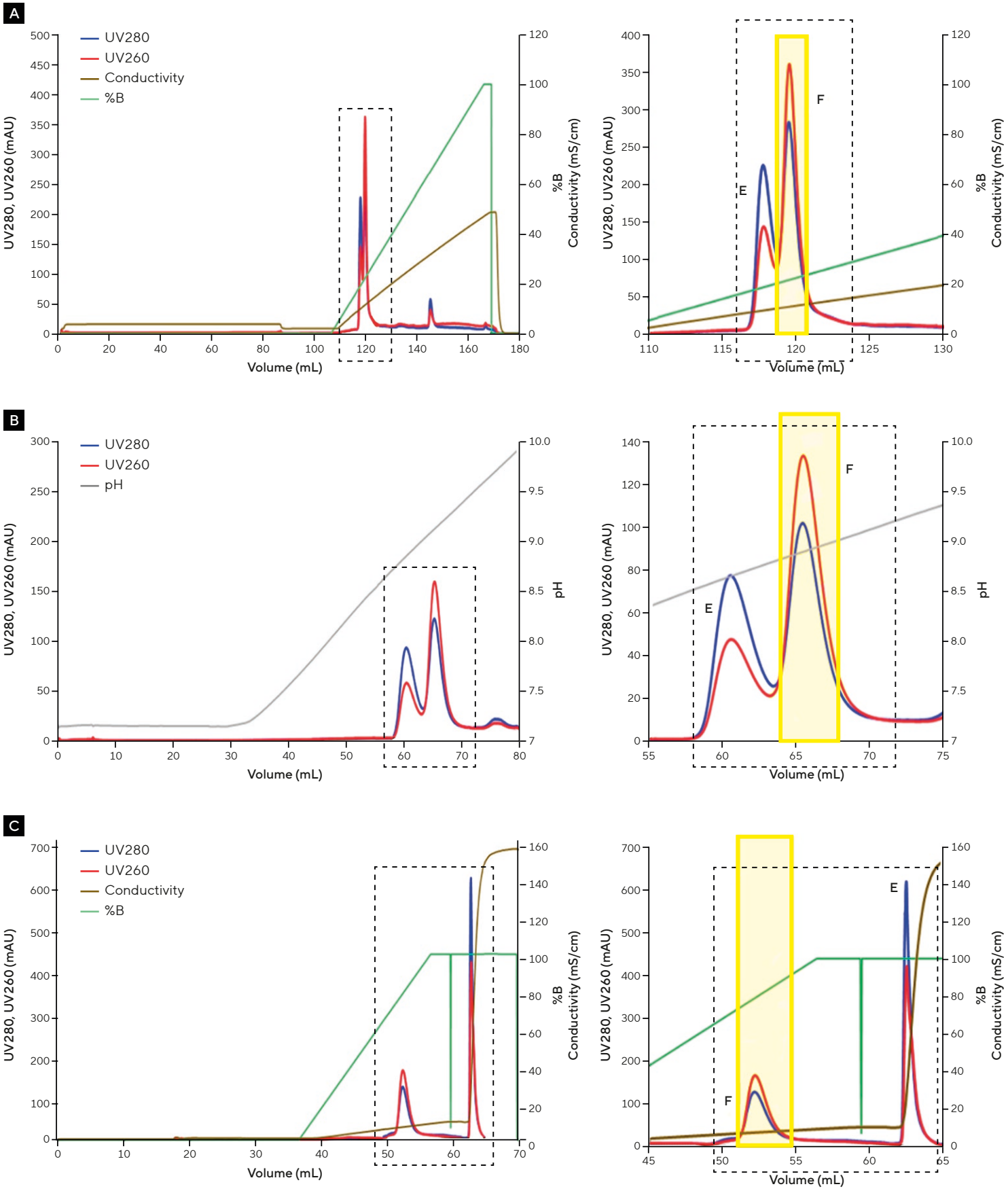

Note. In each chromatogram, the elution peaks are zoomed, the full peak is highlighted in the yellow rectangle. E = empty particle peak, F = full particle peak

Multimodal Chromatography With CIMmultus® PrimaT

Another strategy was used to separate empty and full AAV8 particles using CIMmultus® PrimaT, a weak anion-exchanger coupled with hydrogen bonding and metal chelation effect. In contrast to the other two polishing methods, full AAV8 particles eluted during the gradient, while the empty AAV8 particles only eluted within the final salt strip with 2 M NaCl after the gradient (Figure 4C). The enrichment of full AAV8 particles is similar to the other two polishing methods, approximately 76% (MP) or 75% (PATfix®), respectively (Table 3). Contaminating DNA and proteins are depleted close to the limit of detection of the assays.

Table 3: *Percentage of Full Particles Before Polishing and in the Polishing Full Particle Elution Peak*

Monolith	% Full (PATFix®)	% Full (SamuxMP™)
CIMmultus® SO3	34	25±2
CIMmultus® QA	78.8±0.6	73.4±2
CIMmultus PrimaS®	93±7	80.9±4
CIMmultus® PrimaT	75.3±0.6	76.1±0.7

Note. Mean (N = 2) ± Std Dev

All three polishing methods were highly effective at separating empty from full AAV particles. Selecting one over the other could be based on the design of the targeted purification step (gradient vs. step elution, for example), cleaning ability for column reuse, AAV serotype, different sample preparation strategies (i.e. buffer exchange or dilution), AAV stability at high pH, or performance results (e.g., protein and DNA removal, vg recovery, purity of the full particle fraction). Although the performance of the three monoliths was similar, we selected CIMmultus® PrimaT for scalability studies.

Scale-Up of AAV8 Capture and Polishing Chromatography

After successfully developing an AAV8 capture step using CIMmultus® SO3 and assessing the efficacy of CIMmultus® PrimaT in polishing AAV8 at 1 mL, we performed scale-up capture and polishing runs at 8 mL and 4 mL, respectively. The scale-up process involved maintaining consistent flowrates and step durations per volume of monolith. The experiment was conducted in duplicate, and chromatograms obtained in the two AAV8 capture scale-up runs perfectly overlapped, with no observation of a sample breakthrough during loading (data not shown).

AAV8 particle recoveries and DNA and protein removal obtained during the capture step using CIMmultus® SO3 were comparable at both 1 and 8 mL scales (Figure 5A). The same level of consistency was observed during the scale-up of CIMmultus® PrimaT, as chromatograms of the replicate runs overlapped, and AAV8 recoveries, full particle enrichment and protein removal remained similar at 1 and 4 mL scales (Figure 5B). For scaled-up polishing on the CIMmultus® PrimaT 4 mL, the remaining DNA amount approached the limit of detection of the method, preventing reliable quantification.

The reproducibility observed between the two different monolith scales underscores the success of the development of CIMmultus® SO3 and CIMmultus® PrimaT to capture and polish AAV8. This two-step chromatographic process has demonstrated robustness, reproducibility, and scalability while ensuring high AAV8 recovery, significant enrichment of the full AAV8 population, and effective impurity clearance.

Conclusion

Figure 5: *Comparison of Analytical Results Obtained on the Eluates at Two Monolith Scales for **(A)** AAV8 Capture With CIMmultus® SO3 and **(B)** AAV8 Polishing With CIMmultus® PrimaT*

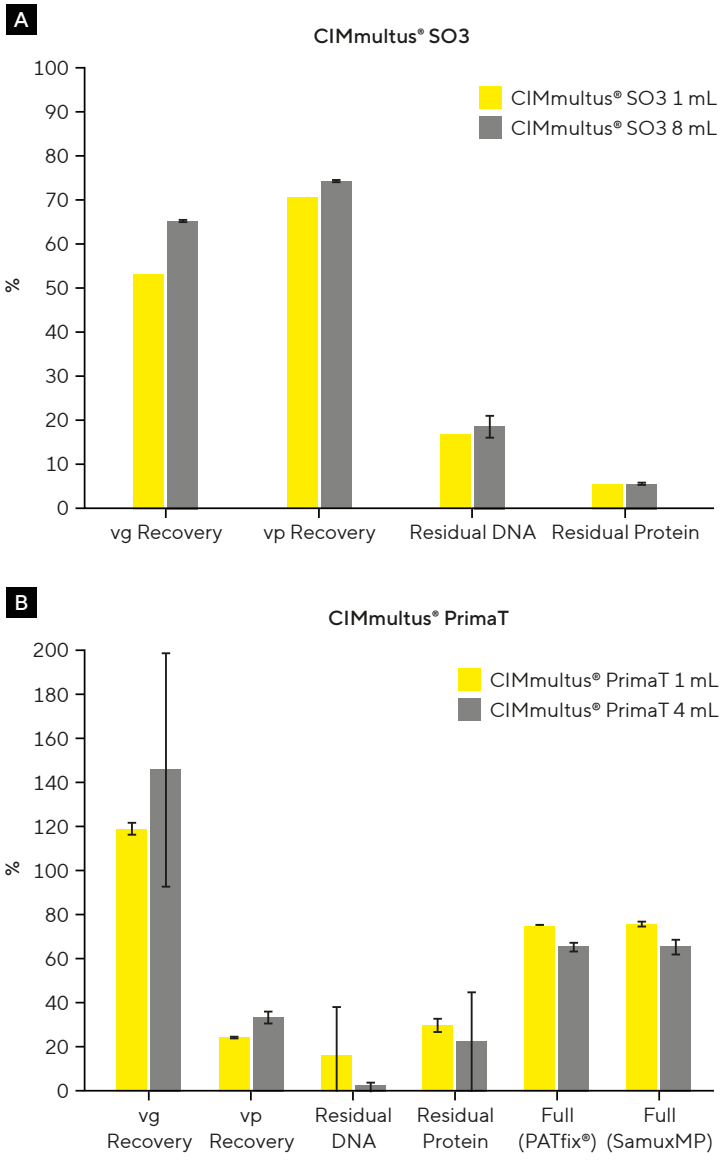

Note. (N = 2 + Std Dev)

Establishing efficient purification processes for AAVs is essential to realize their therapeutic potential. Traditional affinity chromatography and gradient ultracentrifugation offer high selectivity but have limitations, such as costs and serotype dependency for the former, and scalability and productivity for the latter. This application note shows that by leveraging data analytics and screening tools, supported by robust analytical technology, we were able to design an alternative two-step AAV8 purification process based on monolithic chromatography.

Our DoE approach facilitated the screening of optimal conditions to capture AAV8 capsids, while significantly reducing DNA and protein content. Once the capture conditions were defined, we tested three distinct monoliths (CIMmultus® QA, CIMmultus PrimaS®, and CIMmultus® PrimaT) for polishing, each featuring unique binding chemistries. All three exhibited an excellent performance of enriching the full AAV8 particle population by three-fold, while eliminating remaining impurities. We also confirmed the excellent scalability of the method.

These results show that monolithic chromatography represents a robust alternative to the conventional AAV purification process, offering a fast and scalable purification while achieving comparable recovery and purity.

For more information about CIM® monolithic chromatography columns, visit
sartorius.com/monolithic-chromatography

References

1. A. Pupo, A. Fernández, S.H. Low, A. François, L. Suárez-Amarán, R.J. Samulski, AAV vectors: The Rubik's cube of human gene therapy, Mol. Ther. 30 (2022) 3515–3541. https://doi.org/10.1016/j.ymthe.2022.09.015.
2. R.M. Ramamurthy, A. Atala, C.D. Porada, G. Almeida-Porada, Organoids and microphysiological systems: Promising models for accelerating AAV gene therapy studies, Front. Immunol. 13 (2022) 1011143. https://doi.org/10.3389/fimmu.2022.1011143.
3. S.A. Nass, M.A. Mattingly, D.A. Woodcock, B.L. Burnham, J.A. Ardinger, S.E. Osmond, A.M. Frederick, A. Scaria, S.H. Cheng, C.R. O'Riordan, Universal Method for the Purification of Recombinant AAV Vectors of Differing Serotypes, Mol. Ther. Methods Clin. Dev. 9 (2017) 33–46. https://doi.org/10.1016/j.omtm.2017.12.004.
4. J.P. Mendes, M. Bergman, A. Solbrand, C. Peixoto, M.J.T. Carrondo, R.J.S. Silva, Continuous Affinity Purification of Adeno-Associated Virus Using Periodic Counter-Current Chromatography, Pharmaceutics 14 (2022) 1346. https://doi.org/10.3390/pharmaceutics14071346.
5. J.F. Wright, AAV empty capsids: for better or for worse?, Mol. Ther. J. Am. Soc. Gene Ther. 22 (2014) 1–2. https://doi.org/10.1038/mt.2013.268.
6. J. El Andari, D. Grimm, Production, Processing, and Characterization of Synthetic AAV Gene Therapy Vectors, Biotechnol. J. 16 (2021) 2000025. https://doi.org/10.1002/biot.202000025.
7. V. Rajamanickam, C. Herwig, O. Spadiut, Monoliths in Bioprocess Technology, Chromatography 2 (2015) 195–212. https://doi.org/10.3390/chromatography2020195.
8. M. Krajacic, M. Ravnikar, A. Štrancar, I. Gutiérrez-Aguirre, Application of monolithic chromatographic supports in virus research, ELECTROPHORESIS 38 (2017) 2827–2836. https://doi.org/10.1002/elps.201700152.
9. K. Bažec, M. Krašna, A. Mihevc, M. Leskovec, A. Štrancar, M. Tajnik Sbaizero, Optimization of rAAV capture step purification using SO3 monolith chromatography, ELECTROPHORESIS 44 (2023) 1943–1952. https://doi.org/10.1002/elps.202300104.
10. R. Žigon, M.T. Sbaizero, I.P. Koshmak, V. Fujs, M. Leskovec, A. Štrancar, Roadmap to success in AAV purification. In-process control, high throughput & novel column modalities as necessary means for control over scalable AAV process, Cell Gene Ther. Insights (2022). https://doi.org/10.18609/cgti.2022.192.
11. A. Nascimento, T.Q. Faria, F. Bollmann, M. Noverraz, G. Pressac, A. Roldão, C. Peixoto, R.J.S. Silva, Purification of AAV8 through a scalable two-step monolithic chromatography approach, Journal of Chromatography A 1740 (2025), 465586. https://doi.org/10.1016/j.chroma.2024.465586
12. M. Fueger, Y. Jin, A. Thiefes, M. Szelwicki, Sartoclear® Depth Filters for the Clarification of AAV. Application Note, Sartorius, 2024. https://www.sartorius.com/en/application-note-sartoclear-depth-filters-clarification-aav-1610610
13. M. Noverraz, F. Bollmann, P. Nestola, A high-throughput and automated method for AAV tangential flow filtration process development. Application Note, Sartorius, 2024. https://www.sartorius.com/resource/static/celum/295378/Crossflow-System-for-AVV-Purification-Application-Note-en-B.pdf

Germany
Sartorius Stedim Biotech GmbH
August-Spindler-Strasse 11
37079 Goettingen
Phone +49 551 308 0

USA
Sartorius Stedim North America Inc.
565 Johnson Avenue
Bohemia, NY 11716
Toll-Free +1 800 368 7178

For more information, visit
sartorius.com/monolithic-chromatography

Status: 12 | 2024